

## Wave Refraction in Negative-Index Media: Always Positive and Very Inhomogeneous

P. M. Valanju,<sup>1,2</sup> R. M. Walser,<sup>2</sup> and A. P. Valanju<sup>2</sup>

<sup>1</sup>*Fusion Research Center, University of Texas at Austin, Austin, Texas 78712*

<sup>2</sup>*Center for Electromagnetic Materials and Devices, University of Texas at Austin, Austin, Texas 78758*

(Received 12 September 2001; published 19 April 2002)

We present the first treatment of the refraction of physical electromagnetic waves in newly developed negative index media (NIM), also known as left-handed media (LHM). The NIM dispersion relation implies that group fronts refract positively even when phase fronts refract negatively. This difference results in rapidly dispersing, very inhomogeneous waves. In fact, causality and finite signal speed always prevent negative wave signal (not phase) refraction. Earlier interpretations of phase refraction as “negative light refraction” and “light focusing by plane slabs” are therefore incorrect, and published NIM experiments can be explained without invoking negative signal refraction.

DOI: 10.1103/PhysRevLett.88.187401

PACS numbers: 78.20.Ci, 41.20.Jb, 42.15.Dp, 42.25.Bs

Recently developed artificial media with simultaneously negative real parts of frequency dependent dielectric constant  $\epsilon(\omega)$  and permeability  $\mu(\omega)$  have received much attention in journals [1–5] and press [6]. The main interest in these media is in the frequency range (Fig. 1a), where the real part of the phase refractive index  $n_p(\omega) \equiv [\mu\epsilon]^{1/2}$  is negative and the loss is small ( $\text{Im}[n_p] > 0$ ). In order to avoid confusion with circular polarization media, we call them NIM (negative-index media) rather than left-handed media (while PIM = positive index media). The electromagnetic properties of NIMs, which do not occur naturally, take us into new territory, where even familiar concepts must be handled carefully. Most importantly, we point out that at a PIM-NIM interface, one must consider group—rather than just phase—propagation and refraction, because the refraction angles of phase velocity  $\vec{v}_p = \omega/\vec{k}$  and group velocity  $\vec{v}_g = d\omega/d\vec{k}$  (= total energy flux/total energy density) have opposite signs. It is well known [7–10] that, in a dispersive medium (like NIM), it is the group rather than the phase velocity that gives the direction and magnitude of the total energy flow for physically interesting signal-carrying waves. The concept of group refractive index  $n_g$  is widely used [11,12] to distinguish between phase and group refraction in dispersive media such as optical fibers and plasmas. We show that  $n_g$  is positive in NIM, and hence all interpretations of phase refraction as “negative light refraction” and “light focusing by plane slabs” [1–6] are incorrect. Further, we argue that, in general, causality and finite signal speed would be violated if any physically realizable wave (signal) suffered “negative refraction.”

The NIM dispersion relation requires overlapping resonances of  $\mu(\omega)$  and  $\epsilon(\omega)$  [see Eqs. (1) and (2) of [4]]. The narrow, low-loss NIM region of main interest is above the two resonance frequencies, where the real parts of both  $\mu$  and  $\epsilon$  are simultaneously negative and their imaginary parts are small, leading to  $\text{Re}[n_p(\omega)] < 0$  and a small  $\text{Im}[n_p(\omega)] > 0$  (region III in Fig. 1a). The low-loss requirement excludes the anomalous dispersion region near the resonances, to which our causality argu-

ments and results can be extended following Brillouin [8]. For simplicity, here we consider only the low-loss region of interest, where  $\text{Re}[dn_p/d\omega] > 0$  even though  $\text{Re}[n_p] < 0$ . The narrow, low-loss resonances also imply  $|\delta n_p/n_p| \gg |\delta\omega/\omega|$ .

In order to see the difference between the signs of phase and group refraction at a PIM-NIM interface and show that  $n_g$  is positive in NIM, consider a quasimonochromatic plane wave with a frequency spectrum  $f(\omega)$  of nonzero width  $\delta\omega$ . Let all wave vectors  $\vec{k}(\omega)$  be in the  $xz$  plane, and the electric field  $\vec{E}$  in the  $y$  direction (treatment of the other polarization is similar). Let the wave be incident from vacuum (a PIM) at an angle  $\theta_i$  onto a plane NIM surface at  $z = 0$  (Fig. 1b and 1c). Matching the PIM-NIM boundary conditions for each  $\omega$  component at  $z = 0$  gives the complex analytic solution [13] of the linear wave equation on the NIM side:

$$E(t, x, z) = \int d\omega f(\omega) T(\omega, \theta_i) e^{i(\omega t - k_x x - k_z z)},$$

$$k_x = \frac{\omega}{c} s, \quad k_z = \frac{\omega}{c} \sigma \sqrt{n_p(\omega)^2 - s^2}, \quad (1)$$

$$s = \sin\theta_i,$$

where  $\text{Re}[E]$  gives the fast oscillating electric field,  $|E|$  gives the slowly varying envelope,  $c$  is the speed of light in vacuum, and  $T(\omega, \theta_i)$  is the transmission coefficient. The surfaces of constant phase of  $E$  are the phase fronts and those of constant  $|E|$  are the modulation (group) fronts. To avoid irrelevant complications, we will set  $T \approx 1$  for small  $\theta_i$  by assuming  $\epsilon \approx \mu$  (vacuum matching). The sign  $\sigma = \pm 1$  of the square root is chosen to be positive for PIM and negative for NIM, so that, across the PIM-NIM boundary,  $k_z$  changes sign while  $k_x$  is continuous to satisfy the boundary conditions. Note that  $\text{Re}[n_p] < 0$  and  $\text{Im}[n_p] > 0$  inside the square root for NIM, so that  $\sigma < 0$  for NIM yields the correct  $\exp[-k_{zi}z]$  with ( $k_{zi} \equiv \text{Im}[k_z] > 0$ ) as required by the Sommerfeld condition [7] that all fields must vanish at  $z \rightarrow +\infty$ .

For slowly modulated waves (small  $\delta\omega/\omega$ ) the integral in Eq. (1) can be evaluated with good accuracy by noting that the constructive interference is strongest where the phase of the integrand is stationary [7]. The locus of such points is the group front normal to the group velocity  $v_g$ ,

$$E(t, x, z) = 2 \cos[\delta \partial_\omega g(\omega)] e^{ig(\omega)} \text{ at } \omega = \omega_c, \text{ where } g(\omega) = \omega t - k_x(\omega)x - k_z(\omega)z. \quad (2)$$

The group front is the locus of points where the argument of the cosine is zero, i.e.,  $t - x \partial_\omega k_x - z \partial_\omega k_z = 0$ . Even for more general  $f(\omega)$  of narrow width, the group front is given by the stationary phase condition  $\partial_\omega g(\omega) = 0$ , i.e.,

$$0 = ct - xs - zb, \text{ with } s \equiv \sin\theta_i, \text{ and } b \equiv \sigma \left[ \sqrt{n_p^2 - s^2} + \left( \omega \frac{dn_p}{d\omega} \right) \frac{n_p}{\sqrt{n_p^2 - s^2}} \right]. \quad (3)$$

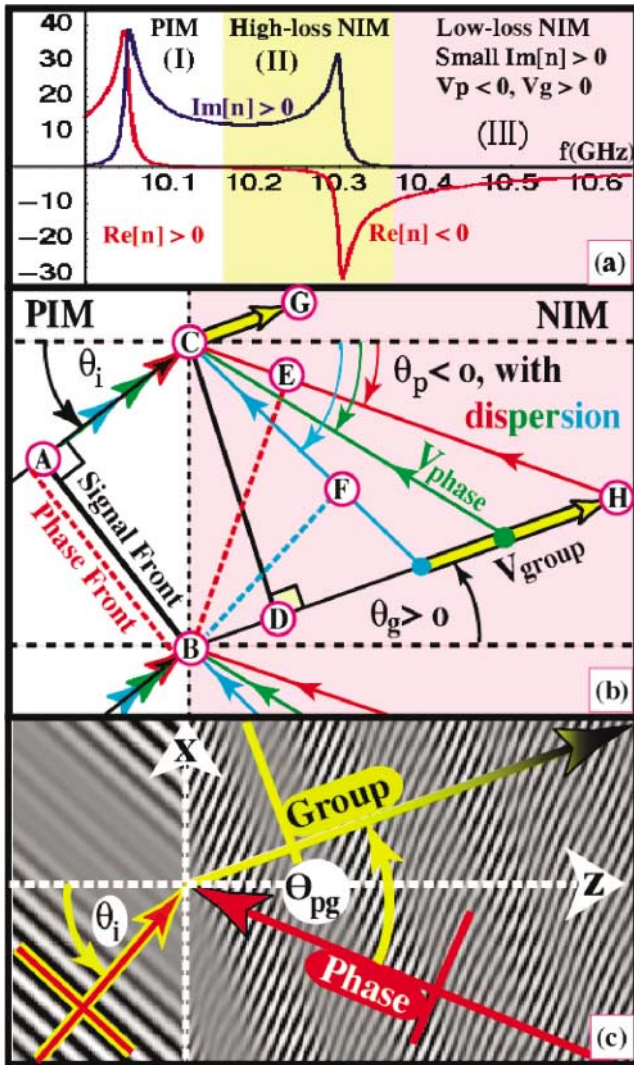


FIG. 1 (color). (a)  $n_p(\omega)$  for parameters in Ref. [4]. The low-loss NIM region (III) above two resonances has negative real parts of  $\epsilon$ ,  $\mu$ , and hence  $n_p$ , small imaginary parts, and  $\text{Re}[n_g] > 0$ . The anomalous dispersion region (II) is of less practical interest. (b) Negative and positive refractions of  $v_p$  and  $v_g$  in NIM. Three  $\omega$  components are shown. (c) Density plot of  $\text{Re}[E(t, x, z)]$  showing phase fronts (sharp bands), and group fronts (wider gray bands). Note signal dispersion at large  $z$  due to  $n_d$ , and large  $\theta_{pg}$  between phase and group fronts.

i.e., to the energy flow direction [9,10]. Since here we are concerned with wave refraction and dispersion rather than absorption, we temporarily neglect the small imaginary part of  $n_p(\omega)$ . The direction of the group front can be seen by restricting  $f(\omega)$  to the simple case of two delta functions at adjacent frequencies  $\omega_c \pm \delta$ , so that

This group front moves at a positive angle  $\theta_g$  to the surface normal ( $z$  axis) given by the “group Snell’s law”

$$\tan(\theta_g) = \frac{(\partial_\omega k_x)}{(\partial_\omega k_z)} = \frac{\sin\theta_i}{b} > 0, \quad (4)$$

$$n_g(\theta_i) \equiv \frac{\sin\theta_i}{\sin\theta_g} > 0.$$

For small  $\theta_i$  the group refractive index reduces to

$$n_g \approx n_p + \omega \frac{dn_p}{d\omega} = \frac{d(\omega n_p)}{d\omega}. \quad (5)$$

Since proximity to narrow resonances is essential for realizing the low-loss NIM, the fractional variation  $\text{Re}[\omega dn_p/d\omega] > 0$  always dominates  $\text{Re}[n_p] < 0$ . Therefore  $\text{Re}[b]$ ,  $\text{Re}[\theta_g]$ , and  $\text{Re}[n_g]$  are positive for low-loss NIM—even when  $\sigma$  and  $\text{Re}[n_p]$  are negative. For example, at 10.5 GHz, the two-resonance NIM dispersion relation (Fig. 1a) with  $\epsilon$ ,  $\mu$ , and parameters from Ref. [4] gives  $n_p = -3.665 + i0.0906$ ,  $n_g \equiv d(\omega n_p)/d\omega = 186.443 - i6.996$ , and the “dispersion index”  $n_d \equiv d(\omega n_g)/d\omega = -14288.6 + i890.65$ . The wave disperses due to  $n_d$  and decays due to all imaginary parts, consistent with Kramers-Kronig relations [14].

The generality of positive signal refraction can be understood from a simple physical argument. Assume that Fig. 1b represents a signal front causally moving from  $BA$  to  $BC$  to  $BE$ . For this, the local signal would have to travel from  $A$  to  $C$  to  $E$  in zero time (equal to the time of travel from  $B$  to  $B$ ), i.e., at infinite speed. Since this is nonphysical, no physical signal or energy front can travel forward and negatively refract in the “NIM” fashion ( $BA$  to  $BC$  to  $BE$ ) at the interface of any two media. Unlike group fronts, phase fronts (dotted lines in Fig. 1b) refract at  $\theta_p < 0$  in NIM. However, they go backwards, and they do not represent causal energy flow.

The ray diagrams and arrows in Refs. [1–5] do not correctly show either the positive refraction angle of the forward propagating group fronts or the backward propagation direction of the negatively refracted phase fronts. Ray diagrams must indicate energy propagation, i.e., group fronts that arise from the constructive interference of

different phase components [11]. Physical rays (normal to group fronts) must refract positively and go forward, as shown in Fig. 1c. The large difference between phase and group refraction in NIM generates very inhomogeneous waves [7,9] that disperse rapidly (Fig. 1c). This can be seen in the stationary phase approximation to Eq. (1) for an incident Gaussian pulse  $f(\omega) = \exp\{-[(\omega - \omega_0)/\delta]^2\}$

$$E(t, x, z) \approx \sqrt{\frac{2}{\phi_{ww}}} \exp\left[\phi_0 - \frac{\phi_w^2}{2\phi_{ww}}\right], \text{ where } \phi(\omega) = -\left[\frac{\omega - \omega_0}{\delta}\right]^2 + i(\omega t - k_x x - k_z z), \quad (6)$$

and  $\phi_0 = \phi(\omega_0)$ ,  $\phi_w = \partial_\omega \phi(\omega)$ , and  $\phi_{ww} = \partial_\omega^2 \phi(\omega)$ , all evaluated at the central frequency  $\omega = \omega_0$ . This result follows from calculating the small shift of the stationary phase point  $\partial_\omega \phi(\omega) = 0$  from the central  $\omega_0$  to order  $\delta^2$ . Taylor expansion, around  $\omega_0$ , of  $n_p(\omega)$  in  $\phi_w$  and  $\phi_{ww}$  shows the positive group refraction direction and also the effects of NIM dispersion that rapidly spread the pulse out and decrease its peak intensity as  $z$  increases (Fig. 2). After refraction by NIM, the waves have large angles  $\pi - \theta_{pg}$  between group and phase propagations (Fig. 1c), starting with  $\pi$  for normal incidence. Such inhomogeneous waves disperse rapidly. For clarity in Figs. 1–3, we have suppressed the reflected waves and used much smaller  $n_g$  and  $n_d$  than the NIM of Ref [4].

We have done a similar calculation [15] for a slightly modulated spherical wave starting from a point source in vacuum ( $n_p = 1$ ) and crossing a plane surface into a NIM with  $n_p(\omega) = -1$  and  $\omega dn_p/d\omega > 0$  at the central wave frequency. The results plotted in Fig. 3 show where the dispersing phase fronts (red and blue curves) constructively interfere to produce a diverging group front (black and white amplitude contours) with large angles between refracted  $\vec{v}_g$  and  $\vec{v}_p$ . Further, for a phase ray starting in PIM at a distance  $d_i$  and angle  $\theta_i$  from the interface, using the phase Snell’s law with  $n_p(\omega) < 0$ , yields the “phase focusing distance”  $d_p(\theta_i, \omega)$  (see Fig. 3b)

$$d_p(\theta_i, \omega) = d_i \sqrt{n_p(\omega)^2 + [n_p(\omega)^2 - 1] \tan^2 \theta_i}. \quad (7)$$

Thus the perfect lens of Ref. [5] has large spherical as well as chromatic aberrations even for phase rays. This lack of aberration-free focusing of even phase rays by plane NIM can also be seen from Fermat’s least-time principle. There

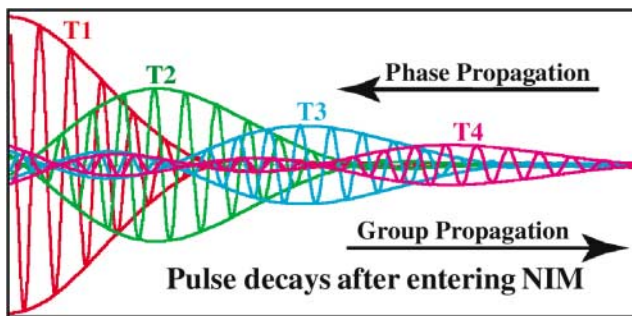


FIG. 2 (color). Dispersion and decay of the forward traveling signal envelope ( $|E|$ ) at four successive times ( $T1-T4$ ), after entering NIM along the  $z$  axis of Fig. 1c. Only the NIM region is shown for clarity. The faster-varying phase carrier waves, i.e.,  $\text{Re}[E]$  shown inside the envelope, travel backward while the envelope travels forward and decays due to NIM dispersion.

is in general only one phase ray joining any two points on two sides of a plane boundary because the net optical path length has only one extremum, i.e., multiple rays starting from a point cannot be focused by a plane PIM-NIM interface to one point. The only singular exception is for the nonphysical case of  $n_p(\omega) = -1$  with  $\omega dn_p/d\omega$  strictly zero for all  $\omega$ . For all real NIM, including the physical  $n_p = -1$  dispersive case, the signal never focuses but instead diverges and disperses. Note that the Sommerfeld condition negates superlensing [5], i.e., the amplification of evanescent modes in the semi-infinite region  $z > 0$  of passive NIM that has no latent energy or a source of power to amplify a wave. Therefore, perfect lenses [5] neither focus nor provide superlensing.

The strongly dispersed, rapidly decaying waves in NIM can tunnel through only finite, optically small NIM devices such as those used in experiments [3,4] so far. Such tunneling is not well represented by geometrical ray optics. For calculating the wave tunneling, both decaying and growing exponentials must be used inside the finite-width slab. Note that this does not contradict our earlier statements about evanescent waves in semi-infinite NIM slabs,

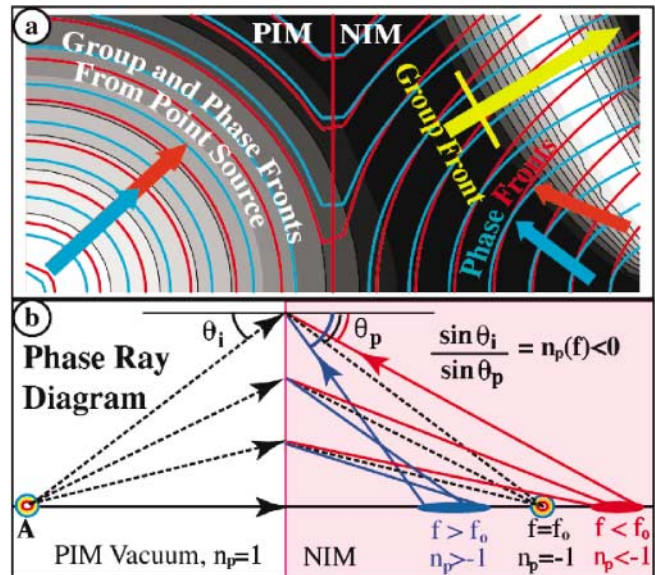


FIG. 3 (color). Causality precludes the perfect superlens of [5]. (a) Density plot of  $|E(t, x, z)|$  shows how the modulation envelope does not focus. Surfaces of constant phase are superimposed in blue and white, and are seen to refract differently in NIM. (b) Even phase rays do not focus to a point in NIM, unless  $n_p(\omega) = -1$  for all  $\omega$ , which is nonphysical (violates causality).

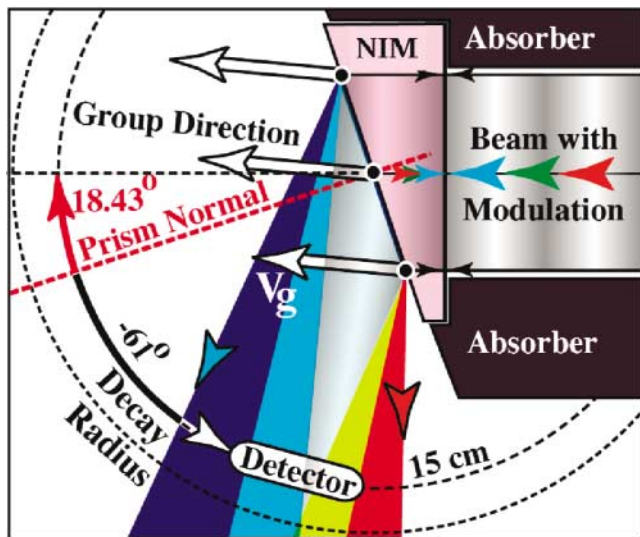


FIG. 4 (color). Simulation of the  $18.43^\circ$  NIM prism experiment with parameters given in Ref [4]. Intensity disperses beyond the near-field triangular overlap region of all frequencies.

and is required for solving the wave equation in finite slabs made from any material. A Laplace transform method has to be used for the propagation of a finite pulse through a finite aperture [15]. The results (Fig. 4) are qualitatively similar to those for infinite apertures, showing the large angle ( $\theta_{pg} \approx 84^\circ$ ) between the output signal  $\vec{v}_g$  and the average phase velocity  $\langle \vec{v}_p \rangle$ . The resulting inhomogeneous wave cannot be regarded as a “negatively refracted beam” because it disperses rapidly along the direction of  $\langle \vec{v}_p \rangle$ . In the NIM media of Refs. [3,4], the dispersive signal loss is further enhanced by the large impedance mismatch with vacuum ( $\epsilon \neq \mu$ ), and the direct loss is due to the imaginary part of  $n_p$ . We expect the intensity to decrease with distance, negating the interpretation of the data in Ref. [4] in terms of a propagating output beam that was negatively refracted by the NIM prism. We interpret the angular intensity profile observed at the short distance of  $15 \text{ cm} \approx 5\lambda$  as near-field effects. We also predict larger attenuation for the NIM case as compared to the teflon case. We cannot verify this because the data presented in Fig. 3 of Ref. [4] are without an absolute scale. Many other potentially misleading issues, such as material anisotropy, edge diffraction, etc., need to be fully addressed before applying geometrical optics to such NIM prisms.

In conclusion, we have shown that causality and finite signal speed preclude negative refraction for any waves incident on any material, including NIM. The NIM dispersion implies positive group refraction even when phase refraction is negative, and causes large angles  $\theta_{pg}$  between phase and signal fronts and creates inhomogeneous waves that rapidly decay, during and after passage through NIM. The strong distortion of the signal puts severe bounds on

the bandwidth of the information that can be transmitted through NIM devices. Negative refraction ray diagrams in all earlier literature do not represent the correct positive wave (i.e., signal) refraction by NIM.

We acknowledge useful discussions with Professor E. C. G. Sudarshan, Professor M. E. Oakes, Dr. R. Chatterjee, and acknowledge partial funding from Texas TDT Grant No. 003658-0849-1999, DARPA-FAME Grant No. MDA-972-98-1-0009, and the Industry Associates of the UT-Center for Electromagnetic Materials and Devices.

- [1] V. G. Veselago, *Sov. Phys. Usp.* **10**, 509 (1968). The arrows shown on what are phase rays in this and Refs. [2–6] all point the wrong (forward) direction in the NIM region.
- [2] D. R. Smith and N. Kroll, *Phys. Rev. Lett.* **85**, 2933 (2000).
- [3] D. R. Smith, W. J. Padilla, S. Schultz, D. C. Vier, and S. C. Nemat-Nasser, *Phys. Rev. Lett.* **84**, 4184 (2000).
- [4] R. A. Shelby, D. R. Smith, and S. Schultz, *Science* **77**, 292 (2001). In our Figs. 1a and 4, we have used their Eqs (1) and (2) for  $\mu(\omega)$  and  $\epsilon(\omega)$  with their parameters  $f_{mp}$ ,  $f_{mo}$ ,  $f_{ep}$ ,  $f_{eo}$ , and  $\gamma$ .
- [5] J. B. Pendry, *Phys. Rev. Lett.* **85**, 3966 (2000).
- [6] We cite here only a small fraction of news articles about LHM: J. B. Pendry, *Phys. World* **14**, 47 (2001); M. C. C. Wiltshire, *Science* **292**, 77 (2001); J. Mullins, *New Sci.* **170**, 35 (2001); P. F. Schewe and B. Stein, *AIP Phys. Bull. Phys. News* **476** (2000); A. Jones, *NSF News*, 21 March 2000; R. C. Johnson, *EE Times*, 8 May 2001; J. Achenback, *Washington Post*, 22 March 2000, p. A13; K. McDonald, *UCSD News Release*, 21 March 2000.
- [7] M. Born and E. Wolf, *Principles of Optics* (Cambridge University Press, Cambridge, U.K., 1980), Appendix III and p. 561.
- [8] L. Brillouin, *Wave Propagation and Group Velocity* (Academic Press, New York, 1960).
- [9] L. D. Landau, E. M. Lifshitz, and L. P. Pitaevskii, *Electrodynamics of Continuous Media* (Pergamon Press, 1984), Chap. IX.
- [10] T. H. Stix, *Waves in Plasmas* (AIP, New York, 1992), Chap. 4, Eq. (27).
- [11] For group refractive index, see C. O. Hines, *J. Geophys. Res.* **56**, 63 (1951); **56**, 197 (1951); **56**, 207 (1951); **56**, 535 (1951); P. L. Auer, H. Hurwitz, Jr., and R. D. Miller, *Phys. Fluids* **56**, 501 (1958); R. A. Helliwell, *Whistlers and Related Ionospheric Phenomena* (Stanford University Press, Stanford, 1965), p. 40.
- [12] D. R. Goff, *Fiber Optic Reference Guide: A Practical Guide to the Technology* (Focal Press, Boston, 1999).
- [13] D. Gabor, *J. Inst. Elect. Eng.* **93**, 429 (1946); J. R. Klauder and E. C. G. Sudarshan, *Fundamentals of Quantum Optics*, Ch. 1 (Benjamin, New York, 1968).
- [14] J. D. Jackson, *Classical Electrodynamics* (Wiley, New York, 1973).
- [15] Details of the straightforward but tedious spherical wave and prism calculations for NIM are not critical to arguments in this paper, and will be given elsewhere.